Petroleum Science 20 (2023) 769–775

Contents lists available at ScienceDirect

Petroleum Science

journal homepage: www.keaipublishing.com/en/journals/petroleum-science

Original Paper

Resin composition: An indicator of oil maturity as revealed by fourier transform ion cyclotron resonance mass spectrometry

Tian Liang [a, b, c], Zhao-Wen Zhan [a, b], Guo-Xiang Wang [a, b, c], Yan-Rong Zou [a, b, *]

[a] State Key Laboratory of Organic Geochemistry, Guangzhou Institute of Geochemistry, Guangzhou, Guangdong, 510640, China
[b] CAS Center for Excellence in Deep Earth Science, Guangzhou, Guangdong, 510640, China
[c] University of Chinese Academy of Sciences, Beijing, 100049, China

ARTICLE INFO

Article history:
Received 13 March 2022
Received in revised form
18 July 2022
Accepted 15 September 2022
Available online 20 September 2022

Edited by Teng Zhu and Jia-Jia Fei

Keywords:
Resin
Pyrolysis
FT-ICR MS
Heteroatom compound
Maturity
DBE

ABSTRACT

A pyrolysis experiment was carried out on a Dongying Depression kerogen sample to separate the resin from the oil. Fourier transform ion cyclotron resonance mass spectrometry (FT-ICR MS) with a positive-ion detector was used to detect the relative proportional changes in the compounds of the resin. During the whole pyrolysis experiment, the relative ratio of resin exceed 10% of the soluble component at each temperature point. Five compounds were detected from the resin: N_1, N_1O_1, N_1O_2, O_1, and O_2. To research the changes in the proportions of the compounds during pyrolysis clearly, these five compounds were divided into three classes: N_1, N_1O_x, and O_x. The N_1 class has the largest proportion in resin at the beginning of the pyrolysis, while O_x class has the least proportion. And the relationship between the number and the molecular mass of three classes compound was researched. With increasing maturity, the proportion of N_1 and the N_1O_x class decreased rapidly, while the O_x class increased slowly. Through researching these resin compounds, it was found that an inversion in the proportions of above three compounds appeared at the end of the oil window. At the same time, we found that the DBE and carbon number of resin compounds have changed obviously during the pyrolysis: the DBE increased, while the carbon number decreased significantly. And the details of the change of each compound have been researched. This research extends our knowledge of judging the maturity of crude oil during the pyrolysis through the characteristics of compounds in resin and provides the new index based on resin for the evaluation of thermal evolution stage and hydrocarbon generation capacity of source rocks.

1. Introduction

Since researchers began to separate petroleum components, numerous studies have focused on petroleum composition [saturates, aromatics, resins, and asphaltenes (SARA)] (Jewell et al., 1972). Resin is a macromolecular non-hydrocarbon compound with an aromatic heterocyclic structure that can dissolve in organic reagents, and forms a substantial proportion of petroleum (Jewell et al., 1974). Compared with the hydrocarbons in oil, resin has a yellow to dark brown oily appearance at room temperature. Furthermore, there are fewer aromatic and naphthenic aromatic hydrocarbon molecules in resin. Many components in resin contain the heteroatomic functional groups, and these heteroatoms replace the carbon atoms in the aromatic rings. According to previous study, there are three main types of heteroatom compounds in resin: oxygen, nitrogen, and sulfur compounds (Strachan et al., 1989). Although these three elements (oxygen (O), nitrogen (N), and sulfur (S)) account for only 2% of petroleum elements, the related compounds account for more than 20% in petroleum, therefore, the composition and distribution characteristics of these compounds have a considerable influence on the nature of petroleum. The relationship between the petroleum components and oil maturity has been studied, and the content of oil compounds during pyrolysis was an important indicator of the maturity changes (Cui et al., 2021). But further research has discovered the evolution mechanisms of biomarkers in saturates and aromatics (Mackenzie et al., 1980; Chen et al., 2011). Asphaltenes also have been researched as the indicators of maturity. However, since the complexity of the compounds in resin components and the

* Corresponding author. State Key Laboratory of Organic Geochemistry, Guangzhou Institute of Geochemistry, Guangzhou, Guangdong, 510640, China.
E-mail address: zouyr@gig.ac.cn (Y.-R. Zou).

https://doi.org/10.1016/j.petsci.2022.09.014

compounds of resin was difficult to be ionized by traditional sass spectrometry (MS), there have been few studies regarding the relationship between resin and petroleum maturity (Nali et al., 2000; Klein et al., 2006; Pereira et al., 2014; Tian et al., 2022). Therefore, a detailed analysis of resin could not only reveal the relationship between resin and petroleum maturity but also provide the essential understanding of resin chemical structures.

Fourier transform ion cyclotron resonance mass spectrometry (FT-ICR MS) analysis has high mass accuracy (< 400 ppb RMS error) and high resolution and is a powerful tool to detect detailed information of petroleum or other complex mixtures (Zhan and Fenn, 2000; Stenson et al., 2002; Li et al., 2012). Utilizing the ICR technology, this test can be used to separate complex compounds and provide an unequivocal molecular formula as $C_cH_hN_nO_oS_s$ (Hughey et al., 2001; Ray et al., 2014). DBE, which can represent the amount of double-band in compound, also been calculated by this analysis (compound: $C_cH_hN_nO_oS_s$, DBE = $c-h/2+n/2+1$) (Oldenburg et al., 2014). Based on the advantages of FT-ICR MS, it is widely used in petroleum testing, in recent years (Li et al., 2010; Mapolelo et al., 2011). Different types of compounds (alkane, aromatic, and polar ONS compounds) have been identified and evaluated using this testing (Kim et al., 2005). Additionally, petroleum maturity can be estimated, and the technique can also be used to analyze the compounds to derive their molecular structure (Kim et al., 2003, 2005; Wan et al., 2017; Wang et al., 2018; Ziegs et al., 2018; Jameel et al., 2019; Vanini et al., 2020). Researchers have also found that the thermal maturity played an important role on the shift of DBE (Hughey et al., 2004; Djokic et al., 2018; Cui et al., 2021). However, there are few studies on this phenomenon in compounds of resin, and most of research focuses on the crude oil, especially the saturated and aromatic compounds in petroleum (Hughey et al., 2004; Wang et al., 2021; Aguiar et al., 2022). In this study, we separated the resin from oils with different maturity to research the changes of its compound DBE and carbon number by FT ICR MS (Hughey et al., 2004; Djokic et al., 2018; Cui et al., 2021).

According to previous research, electrospray ionization (ESI), atmospheric pressure photoionization (APPI), and atmospheric pressure chemical ionization (APCI) are the most commonly used ionization sources (Bae et al., 2010). There are two detection modes of FT-ICR MS. A positive-ion electrospray ionizer is suitable to detect nitrogen compounds, while a negative-ion electrospray ionizer is used to detect acidic compounds and neutral nitrogen compounds in petroleum (Qian, 2001; Qian and Robbins, 2001; Oldenburg et al., 2014). In order to detect more nitrogen-containing compounds and enrich the types of compounds from resin, positive-ion electrospray ionizer was used in this study.

In this study, 11 petroleum samples of different maturities (Easy $\%R_o$ = 0.80–1.98) were obtained through a thermal simulation experiment, and the resin was then separated from the petroleum. The resin samples were analyzed using FT-ICR MS with a positive-ion electrospray to research the compound changes in the resin with increasing maturity and to reveal the indicative significance of these changes regarding petroleum maturity. And the main purpose of this research is to focus on the feasibility of establishing the connection between resin composition and maturity.

2. Sample and experiment

2.1. Sample

The rock sample was collected from Well W161, Dongying Depression, Bohai Bay Basin, at the depth of 1911.9 m. The lithology of the core was mud shale, and the stratum of the sample was Eocene Shahejie Formation. The sample was ground into a powder (approximately 0.075 mm), and the inorganic minerals were removed using hydrochloric acid (6 mol/L) and hydrofluoric acid (40%). After demineralization, the rock powder was extracted using a Soxhlet extractor (in a 50 °C water bath) with a dichloromethane and methanol mixture (93:7 in volume) for 72 h to remove the soluble organic matter, and the pure kerogen powder was collected.

Rock-Eval was used to evaluate the original kerogen, and the basic geochemistry parameters were total organic carbon (TOC) of 40.22%, T_{max} of 436 °C, and hydrogen index (HI) of 714 mg/g TOC. Both the S_2 (287 mg/g TOC) and HI demonstrated that the kerogen had good hydrocarbon-generation potential during the pyrolysis. The maturity of original kerogen was calculated by Eq. (1) (Jarvie et al., 2001):

$$R_o\% = 0.018 \times T_{max} - 7.16 \quad (1)$$

where the T_{max} was detected by Rock-Eval. These parameters indicated that the sample belonged to Type I organic matter, and the basic geochemistry parameters were shown in Fig. 1.

2.2. Experiment and analysis

Artificial pyrolysis was used to prepare a series of resin samples of differing maturities (Pan et al., 2006; Gao et al., 2017; Liang et al., 2020). Easy$\%R_o$ is a simple model to evaluate the maturity of product of artificial pyrolysis (Sweeney and Burnham, 1990). Approximately 100 mg kerogen was sealed in a gold tube (a total of 11 tubes), and the air in the tube was exchanged with argon. Each tube was placed in a separate stainless-steel vessel. All the vessels were placed in one furnace, with a pressure of 50 MPa. The temperature was increased from the ambient temperature to 300 °C over 8 h, maintained at 300 °C for 2 h, and then increased at 2 °C/h to 450 °C. The vessels were removed from the furnace per ten degrees from 350 °C to 450 °C, and a total of 11 temperature point samples were obtained.

The gold tubes were cut open, and the resulting material was extracted using a Soxhlet extractor with a dichloromethane and methanol mixture (93:7) for 72 h. Using a chromatography column,

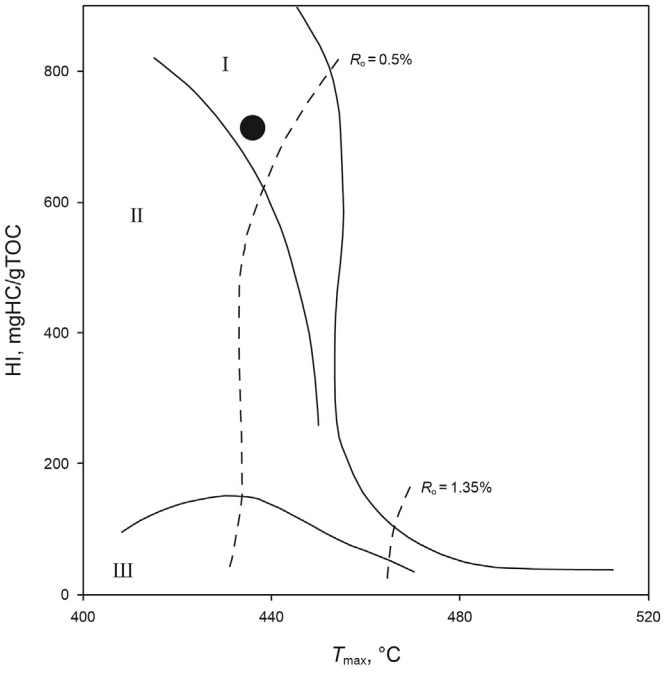

Fig. 1. Diagram of basic geochemical parameters of kerogen.

the soluble organic group was separated into the four SARA components, and the resin was then analyzed.

A SolariX XR FT-ICR MS (Bruker Daltonik GmbH, Bremen, Germany) with a 9.4 T refrigerated actively shielded superconducting magnet (Bruker Biospin, Wissembourg, France) was used for the resin analysis. The resin samples were ionized in the positive-ion mode using an ESI ion source (Bruker Daltonik GmbH, Bremen, Germany). The detection mass range was m/z 150–1,200, and 0.7 s was set as the ion accumulation time. A typical mass-resolving power ($m/\Delta m$ 50%, where Δm 50% is the magnitude of the mass spectral peak full width at half-maximum peak height) was more than 450,000 at m/z 319, and the absolute mass error was less than 0.3 ppm (Jiang et al., 2014).

3. Results and discussion

3.1. SARA faction of soluble organic group

The yields of SARA are shown in Table 1. From the table, the peak of hydrocarbon generation was the maturity of 1.15 Easy%R_o. After this sample point, the yields of saturate and aromatic hydrocarbon decreased with the maturity increased. The yields of resin and asphaltenes reached the peak at the beginning during the pyrolysis (Easy%R_o = 0.86), and after this maturity, the ratio of conversion continued to decrease. This shows that the resin is less supplemented by new substances in the process of hydrocarbon generation, which is more suitable as an indicator for evaluating maturity. Considering the yield of four components of oil (SARA), continued to decrease after this maturity, this maturity also indicated the end of the oil window: after this, all of four components yields decreased with the increasing of maturity. And in Fig. 2, the four proportions were normalized to 100%. The relative ratio of hydrocarbon compounds (saturated and aromatic hydrocarbon) increased from 33.65% to 56.45% over a heating range of 350–410 °C and then gradually decreased to 44.44% (450 °C). In contrast, the maximum proportion of non-hydrocarbon components (resin and asphaltene) was reached at 43.55% (410 °C).

As the object of this research, resin was a significant compound in the soluble organic matter during experimental process, its proportion was always above 15% during the pyrolysis, with the maximum close to 50%. These results indicate that resin is a compound with high yield and stable relative proportions during pyrolysis, and it may be a good indicator of petroleum maturity.

3.2. Molecular mess of the compound

Using FT-ICR MS (positive-ion ESI), the masses of the main compounds were distributed in the interval of 200–800 Da (Dalton, unit of molecular weight) during low maturity, and the range

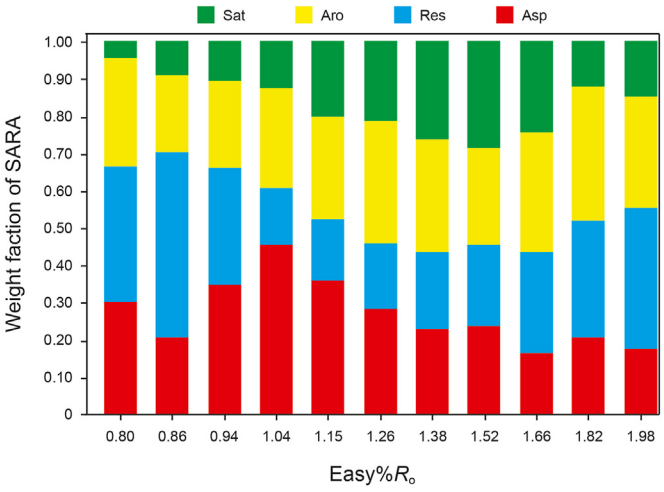

Fig. 2. Diagram illustrating the changes in the yield of soluble organic matter.

changed to 200–400 Da with increasing of Easy%R_o, which was similar to previously researched (Shinn and Robinson, 2001). Furthermore, over the temperature range of 410–450 °C (Easy%R_o > 1.52), the relative proportion of the compound with the molecular weight of 680.47 Da increased. This phenomenon suggested that macro-molecular compounds cracked during pyrolysis, and the compound with 680.47 Da might be more stable than the other compounds under high maturity.

The averaged molecular mass and amount of each compound are shown in Fig. 3, both with a downward trend throughout the experiment. The macro-molecular compounds were broken during pyrolysis, some of them formed smaller molecules, while others combined with asphaltenes and kerogen via condensation (Liao et al., 2015).

There were five nitrogen and oxygen compounds detected by positive-ion ESI FT-ICR MS, i.e., N_1, N_1O_1, N_1O_2, O_1, and O_2. To research the changes in the proportions of the compounds during pyrolysis clearly, these five compounds were divided into three classes: N_1, N_1O_x, and O_x. As Fig. 3 demonstrates, the nitrogen compounds were heavier than O_x, and there was more nitrogen than O_x at the beginning of pyrolysis. With increasing maturity, both the proportions show a decreasing trend until they reached the level of the O_x compounds.

The range of the average molecular mass of the O_x class was 313.60–291.34 Da. In contrast, the averaged molecular masses of the N_1 and N_1O_x compounds were 517.16–271.93 Da and 468.06–309.20 Da, respectively, and the change in the area of the nitrogen compounds was much larger than that of O_x. The amount

Table 1
Soluble organic matters from pyrolysis.

Sample ID	Easy%R_o	Kerogen, mg	Yields of each components, mg/g TOC				Total, mg/g TOC
			S	A	R	A	
W1	0.8	101.49	57.80	50.16	91.36	402.51	601.83
W2	0.86	116.09	113.98	39.19	101.58	437.48	692.23
W3	0.94	116.15	78.35	109.90	96.03	317.94	602.20
W4	1.04	114.71	98.41	118.78	93.37	212.47	523.04
W5	1.15	81.08	117.09	97.37	79.47	138.02	431.95
W6	1.26	115.28	103.04	80.32	66.78	73.60	323.75
W7	1.38	111.94	81.95	61.30	33.84	90.19	267.28
W8	1.52	97.58	72.34	63.51	33.02	78.64	247.50
W9	1.66	116.09	30.93	49.26	22.88	42.90	145.97
W10	1.82	119.31	11.13	36.80	21.54	24.74	94.20
W11	1.98	119.87	10.67	24.83	22.06	14.77	72.32

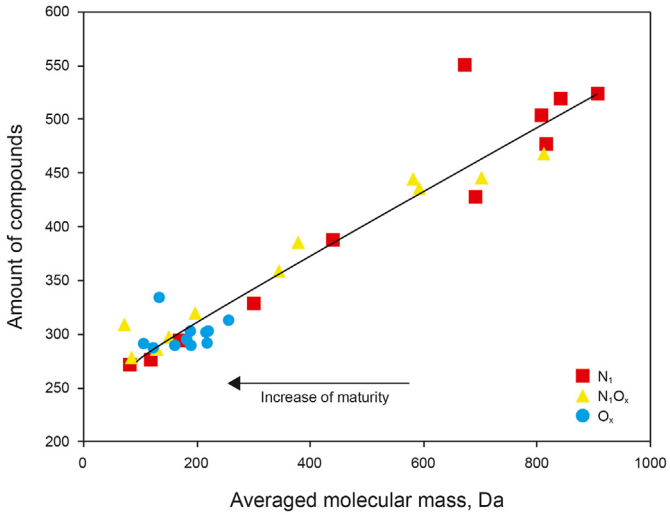

Fig. 3. Variation in the average molecular mass and amount of each compound.

of N_1 decreased from 841 to 81, and the N_1O_x compounds decreased from 813 to 71. From Fig. 3, the five compounds in the resin showed the same characteristics during pyrolysis, the macro-molecular compounds degraded at a low energy, while the small molecules cracked under high maturity. Any of these compounds could serve as effective maturity indicators.

3.3. Relative ratio changes for each compound

The relative proportion of each compound during pyrolysis is shown in Fig. 4. As the highest content in the resin, the N_1 class peak yield was at the maturity of Easy%R_o 1.15. Its proportion increased from 64.91% to 80.72% and then decreased to 38.77% at the end of the pyrolysis. This meant that compounds in the N_1 class had separated from the kerogen in the early stage of oil generation, and after crossing the hydrocarbon generation peak, the N_1 structures gradually broke under high maturity. N_1O_x includes N_1O_1 and N_1O_2, and their proportional changes were similar to each other (Fig. 4). Their relative ratio decreased Easy%R_o was in the range of 0.80–1.15 and increased when Easy%R_o ranged from 1.15 to 1.98. The relative ratio decreased from 28.64% to 12.08%, and finally increased to 21.24%.

At the beginning of the heating process (Esay%R_o = 0.80–0.94), the O_x proportion showed a slight decline from 6.63% to 2.74%, and the amount of the N_1 class increased rapidly (Fig. 4). From then until the experiment was completed, the proportion of the O_x increased from 2.74% to 39.99%. Even though the trend of change in the N_1O_x ratio was synchronous with that of O_x, the O_x content grew more rapidly than the N_1O_x in the later stage. This result indicated that the O_x molecules were more stable than N_1O_x and N_1 at high maturity.

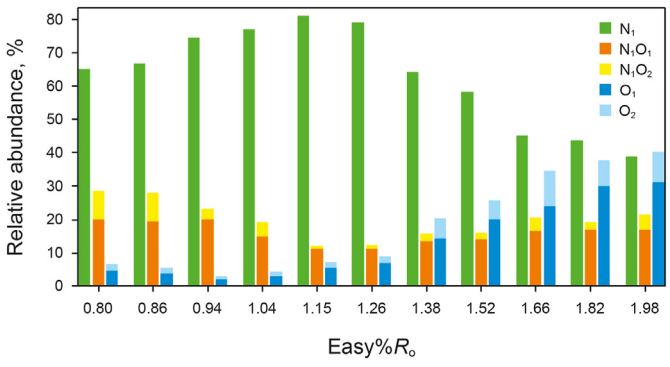

Fig. 4. Illustration of the relative abundance of five compounds in relation to maturity.

Fig. 5 presents a triangular diagram of the relative proportion of the three classes (N_1, N_1O_x, O_x). As is evident from the figure, the curves of the compounds have a significant reversal at Easy%R_o 1.15. This phenomenon indicated that the composition of the resin compounds experiences several clear changes during the process of hydrocarbon generation. These changes constituted a significant inflection point between the resin compositions, which appeared at the end of oil window.

This outcome indicated that the components of the resin are noticeably different around the end of the oil window, which could be an effective indicator of the evolution stage of crude oil. At the completion of the oil window, the amount of N_1 compounds decreased while the O_x compounds increased.

3.4. DBE and carbon number of compounds changes

3.4.1. Changes of total compound

The changes of DBE and carbon number of all of the compounds have been shown in Fig. 6. In the figure, the color close to blue indicates low signal intensity of this compound, while close to red indicates the high content of this compound. In the oil window, the DBE of the compounds in the resin is dominated by 4–5 (Easy%R_o less than 1.26), and while after the oil window, the DBE value of the majority compound quickly rises to 10–15. The carbon number of compounds shows the same changes with DBE. At the beginning of pyrolysis, the carbon number of compounds is generally in the range of 5 to 60, and a large number of compounds with the carbon number more than 25. With the maturity increasing, the signal intensity of macro-molecular compounds (carbon number more than 25) decreases, and the carbon number of the main compound drops below 25 after the oil window. In general, with the increase of maturity, the DBE and carbon number of resin compounds have obvious changes, and this change appears after the oil window

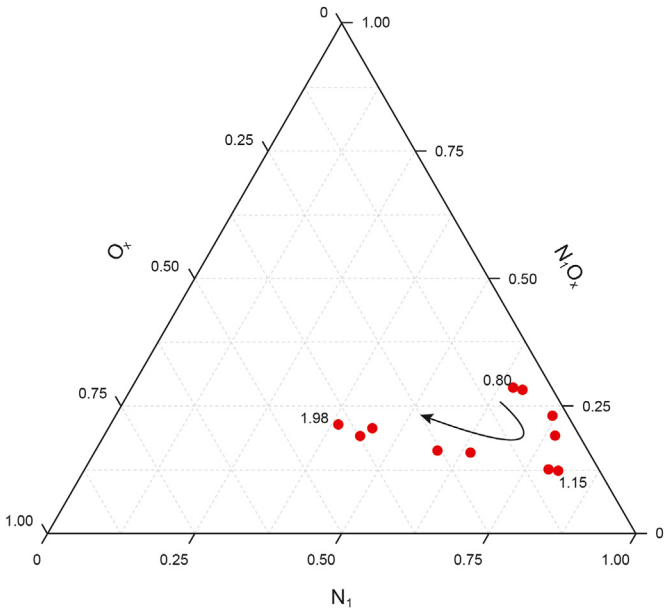

Fig. 5. Triangular plot illustrating the effect if maturity changes on the relative distribution of N_1, N_1O_x, and O_x. [numbers near the data points indicate the oil maturity, curve indicates the increasing trend of oil maturity].

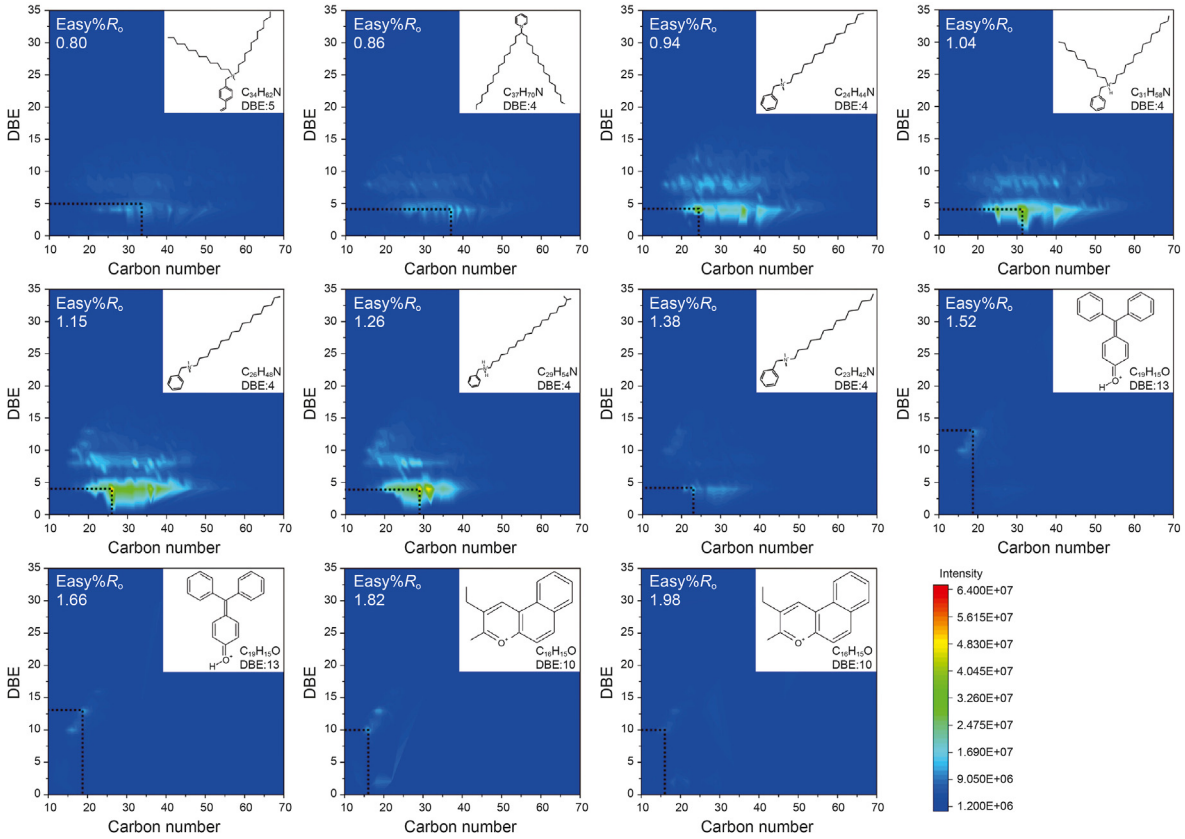

Fig. 6. The abscissa and ordinate in the figure are the carbon number and DBE of total compounds in this research respectively, select the compound with the strongest signal intensity as the representative compound, and its molecular model and formula are shown in the figure.

(Easy%R_o more than 1.26), which is consistent with the reversal phenomenon mentioned above.

In order to research the changes of resin compounds during the evolution process of pyrolysis accurately, we inferred the compound with the strongest signal intensity based on the molecular formula and DBE obtained from the FT ICR MS, and illustrated its molecular structure in the figure (Fig. 6) (PubChem). Near the oil window, the aromatic compounds with long-chain dominate the resin, and most of the compounds are nitrogen compounds. It's just that as the maturity increases, the length of aliphatic chain changes. However, beginning of the maturity of 1.52 (Easy%R_o), compounds with high DBE value in the resin occupy a dominant position, and the signal intensity of oxygen compounds exceeds that of nitrogen compounds. This phenomenon consisted with the changes of DBE and carbon number.

3.4.2. DBE and carbon number changes of each compounds

Fig. 7 illustrated the changes of DBE and carbon number of the compound with the strongest signal in the resin. And we have added five figures of DBE-carbon number changes to the supporting material. As the figure shown (Fig. 7), the carbon number of N_1 compound decreased, while the O_x compound (both O_1 and O_2 compound) increased with the maturity increasing. And the carbon number of N_1O_x compound (N_1O_1 and N_1O_2 compound) reduced slightly at the same time. These changes indicated that the pyrolysis temperature of oxygenates (N_1O_x and O_x) is significantly higher than that of nitrogen-containing compounds (N_1 and N_1O_x): the carbon number of the N_1 compound decreased from the 34 to 16, while both O_1 and O_2 compounds increased from 15 to 19 during the same period. This phenomenon is consistent with the previous conclusion.

As for the changes in DBE, this parameter of four compounds with the strongest signal all showed an increasing trend with increasing maturity until the maturity of 1.82 (Easy%R_o). This phenomenon is due to the strong bonding energy of high DBE compounds containing aromatic rings, so the signal becomes stronger as the maturity increases. Based on these phenomenon, O_x compound exist in various maturity resin (from 0.80 to 1.98), and the structure of this compound is relatively stable than nitrogen compounds. It is a better choice of marker compounds in crude oil research.

4. Conclusions

In this research, FT-ICR MS (with positive-ion electrospray ionizer) was used to analyze the change in the resin compounds during the hydrocarbon generation process of kerogen. And the several conclusions were drawn out:

(1) The hetero-atomic compounds were more stable than the hydrocarbon compounds under high maturity. Compared with hydrocarbons, resin is more suitable for evaluating the maturity of source rocks in high evolution stage;
(2) The relative proportions of N_1O_x, N_1, and O_x in the resin have an obviously reversed at the end of oil window. And three diagrams have been established to describe this phenomenon. This found provides a new index based on resin for the evaluation of thermal evolution stage and hydrocarbon generation capacity of source rocks.
(3) Compared with nitrogen compounds, oxygen compounds showed the higher stability. And it is more suitable for

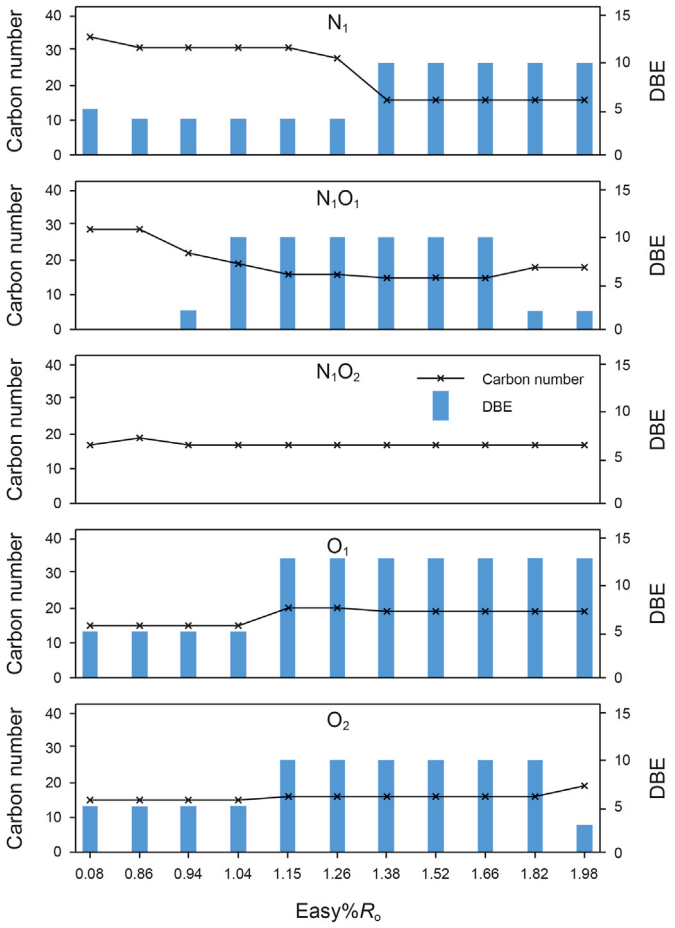

Fig. 7. The changes of DBE and carbon number of each kinds of compounds.

evaluating the stage of highly mature source rocks (especially after the oil window).

Acknowledgements

This work was financially supported by the Strategic Priority Research Program of the Chinese Academy of Sciences (XDA14010102). Thanks to the help of Dr. Wan Nannan, Guangzhou Institute of Geochemistry in drawing of the figure.

Appendix A. Supplementary data

Supplementary data related to this article can be found at https://doi.org/10.1016/j.petsci.2022.09.014.

References

Aguiar, D.V.A., Lima, G.S., Silva, R.R., et al., 2022. Comprehensive composition and comparison of acidic nitrogen- and oxygen-containing compounds from pre- and post-salt Brazilian crude oil samples by ESI (-) FT-ICR MS. Fuel 326, 125129. https://doi.org/10.1016/j.fuel.2022.125129.

Bae, E.J., Na, J.G., Chung, S.H., et al., 2010. Identification of about 30000 chemical components in shale oils by electrospray ionization (ESI) and atmospheric pressure photoionization (APPI) coupled with 15 T fourier transform ion cyclotron resonance mass spectrometry (FT-ICR MS) and a comparison to conventional oil. Energy Fuels 24, 2563–2569. https://doi.org/10.1021/ef100060b.

Chen, Z.H., Ming, Z., Jin, Q., et al., 2011. Distribution of sterane maturity parameters in a lacustrine basin and their control factors: a case study from the Dongying Sag, East China. Petrol. Sci. 8 (3), 290–301. https://doi.org/10.1007/s12182-011-0146-9.

Cui, D., Li, J., Zhang, X., et al., 2021. Pyrolysis temperature effect on compositions of basic nitrogen species in Huadian shale oil using positive-ion ESL FT-ICR MS and GC-NCD. J. Anal. Appl. Pyrolysis. https://doi.org/10.1016/j.jaap.2020.104980, 104980.

Djokic, M.R., Muller, H., Ristic, N.D., et al., 2018. Combined characterization using HT-GC × GC-FID and FT-ICR MS: a pyrolysis fuel oil case study. Fuel Process. Technol. 182, 15–25. https://doi.org/10.1016/j.fuproc.2018.10.007.

Gao, Y., Zou, Y.R., Liang, T., et al., 2017. Jump in the structure of Type I kerogen revealed from pyrolysis and ^{13}C DP MAS NMR. Org. Geochem. 112, 105–118. https://doi.org/10.1016/j.orggeochem.2017.07.004.

Hughey, C.A., Hendrickson, C.L., Rodgers, R.P., et al., 2001. Kendrick mass defect spectrum: a compact visual analysis for ultrahigh-resolution broadband mass spectra. Anal. Chem. 73 (19), 4676–4681. https://doi/abs/10.1021/ac010560w.

Hughey, C.A., Podgers, R.P., Marshall, A.G., et al., 2004. Acidic and neutral polar NSO compounds in Smackover oils of different thermal maturity revealed by electrospray high field Fourier transform ion cyclotron resonance mass spectrometry. Org. Geochem. 35 (7), 863–880. https://doi.org/10.1016/j.orggeochem.2004.02.008.

Jameel, A.G.A., Khateeb, A., Elbaz, A.M., et al., 2019. Characterization of deasphalted heavy fuel oil using APPI (+) FT-ICR mass spectrometry and NMR spectroscopy. Fuel 253, 950–963. https://doi.org/10.1016/j.fuel.2019.05.061.

Jarvie, D.M., Claxton, B.L., Henk, F., et al., 2001. Oil and shale gas from the barnett shale, fort worth basin, Texas. Am. Assoc. Pet. Geol. 10, A100.

Jewell, D.M., Weber, J.H., Bunger, J.W., et al., 1972. Ion-exchange, coordination, and adsorption chromatographic separation of heavy-end petroleum distillates. Anal. Chem. 44 (8), 1392–1395. https://doi.org/10.1021/ac60316a003.

Jewell, D.M., Albaugh, E.W., Davis, B.E., et al., 1974. Integration of chromatographic and spectroscopic techniques for the characterization of residual oils. Ind. Eng. Chem. Fundam. 13 (3), 278–282. https://doi.org/10.1021/i160051a022.

Jiang, B., Liang, Y.M., Xu, C.M., et al., 2014. Polycyclic aromatic hydrocarbons (PAHs) in ambient aerosols from beijing: characterization of low volatile PAHs by positive-ion atmospheric pressure photoionization (APPI) coupled with fourier transform ion cyclotron resonance. Environ. Sci. Technol. 48 (9), 4716–4723. https://doi.org/10.1021/es405295p.

Kim, S., Kramer, R.W., Hatcher, P.G., 2003. Graphical method for analysis of ultrahigh-resolution broadband mass spectra of natural organic matter, the van krevelen diagram. Anal. Chem. 75 (20). https://doi.org/10.1021/ac034415p, 5336-5334.

Kim, S., Stanford, L.A., Rodgers, R.P., et al., 2005. Microbial alteration of the acidic and neutral polar NSO compounds revealed by Fourier transform ion cyclotron resonance mass spectrometry. Org. Geochem. 36 (8), 1117–1134. https://doi.org/10.1016/j.orggeochem.2005.03.010.

Klein, G.C., Angström, A., Rodgers, R.P., et al., 2006. Use of saturates/aromatics/resins/asphaltenes (SARA) fractionation to determine matrix effects in crude oil analysis by electrospray ionization fourier transform ion cyclotron resonance mass spectrometry. Energy Fuels 20 (2), 668–672. https://doi.org/10.1021/ef050353p.

Li, M.W., Chen, D.S., Pan, X.H., et al., 2010. Characterization of petroleum acids using combined FT-IR, FT-ICR–MS and GC–MS: implications for the origin of high acidity oils in the Muglad Basin. Sudan. Org. Geochesm. 41 (9), 959–965. https://doi.org/10.1016/j.orggeochem.2010.03.006.

Li, S.M., Shi, Q., Pang, X.Q., et al., 2012. Origin of the unusually high dibenzothiophene oils in Tazhong-4 Oilfield of Tarim Basin and its implication in deep petroleum exploration. Org. Geochem. 48 (1), 56–80. https://doi.org/10.1016/j.orggeochem.2012.04.008.

Liang, T., Zou, Y.R., Zhan, Z.W., et al., 2020. An evaluation of kerogen molecular structures during artificial maturation. Fuel 265, 116979. https://doi.org/10.1016/j.fuel.2019.116979.

Liao, Y.H., Zheng, Y.J., Pan, Y.H., et al., 2015. A method to quantify C1-C5 hydrocarbon gases by kerogen primary cracking using pyrolysis gas chromatography. Org. Geochem. 79, 49–55. https://doi.org/10.1016/j.orggeochem.2014.12.009.

Mackenzie, A.S., Patience, R.L., Maxwell, J.R., 1980. Molecular parameters of maturation in the Toarcian shales, Paris Basin, France-I. Changes in the configurations of acyclic isoprenoid alkanes, steranes and triterpanes. Geochem. Cosmochim. Acta 44 (11), 1709–1721. https://doi.org/10.1016/0016-7037(80)90222-7.

Mapolelo, M.M., Rodgers, R.P., Blakney, G.T., et al., 2011. Characterization of naphthenic acids in crude oils and naphthenates by electrospray ionization FT-ICR mass spectrometry. Int. J. Mass Spectrom. 300, 149–157. https://doi.org/10.1016/j.ijms.2010.06.005.

Nali, M., Caccialanza, G., Ghiselli, C., et al., 2000. Tmax of asphaltenes: a parameter for oil maturity assessment. Org. Geochem. 31 (12), 1325–1332. https://doi.org/10.1016/S0146-6380(00)00068-1.

Oldenburg, T.B.P., Brown, M., Bennett, B., et al., 2014. The impact of thermal maturity level on the composition of crude oils, assessed using ultra-high resolution mass spectrometry. Org. Geochem. 75, 151–168. https://doi.org/10.1016/j.orggeochem.2014.07.002.

Pan, C.C., Yu, L.P., Liu, J.Z., et al., 2006. Chemical and carbon isotopic fractionations of gaseous hydrocarbons during abiogenic oxidation. Earth Planet Sci. Lett. 15, 70–89. https://doi.org/10.1016/j.epsl.2006.04.013. PubChem (nih.gov). https://pubchem.ncbi.nlm.nih.gov.

Pereira, T.M.C., Vanini, G., Tose, L.V., et al., 2014. FT-ICR MS analysis of asphaltenes: asphaltenes go in, fullerenes come out. Fuel 131, 49–58. https://doi.org/10.1016/j.fuel.2014.04.049.

Qian, K.N., Robbins, W.K., 2001. Resolution and identification of elemental compositions for more than 3000 crude acids in heavy petroleum by negative-ion microelectrospray high-field fourier transform ion cyclotron resonance mass

spectrometry. Energy Fuels 15 (6), 1505–1511. https://doi.org/10.1021/ef010111z.
Qian, K.N., 2001. Reading chemical fine print: resolution and identification of 3000 nitrogen-containing aromatic compounds from a single electrospray ionization fourier transform ion cyclotron resonance mass spectrum of heavy petroleum crude oil. Energy Fuels 15 (2), 492–498. https://doi.org/10.1021/ef000255y.
Ray, P.Z., Chen, H., Podgorski, D.C., et al., 2014. Sunlight creates oxygenated species in water-soluble fractions of Deepwater horizon oil. J. Hzard. Mater. 280 (14), 636–643. https://doi.org/10.1016/j.jhazmat.2014.08.059.
Shinn, J.H., Robinson, R.C., 2001. On the nature and origin of acidic species in petroleum. 1. Detailed acid type distribution in a California crude oil. Energy Fuels 15 (6), 1498–1504. https://doi.org/10.1021/ef010106v.
Strachan, M.G., Alexander, R., Subroto, E.A., et al., 1989. Constraints upon the use of 24-ethylcholestane diastereomer ratios as indicators of the maturity of petroleum. Org. Geochem. 14 (4), 423–432. https://doi.org/10.1016/0146-6380(89)90007-7.
Stenson, A.C., Langding, W.M., Marshall, A.G., et al., 2002. Ionization and fragmentation of humic substances in electrospray ionization fourier transform-ion cyclotron resonance mass pectrometry. Anal. Chem. 74, 4397–4409. https://doi/abs/10.1021/ac020019f.
Sweeney, J.J., Burnham, A.K., 1990. Evaluation of a simple model of vitrinite reflectance based on chemical kinetics. AAPG Bull. 74 (10), 1559–1570.
Tian, Y.K., Jiang, B., Chen, J., et al., 2022. Characterisation by ESI FT-ICR MS of heteroatomic compounds in catalytic hydropyrolysates released from marine crude oil asphaltenes. Org. Geochem. 167, 104391. https://doi.org/10.1016/j.orggeochem.2022.104391.
Vanini, G., Barra, T.A., Souza, L.M., et al., 2020. Characterization of nonvolatile polar compounds from Brazilian oils by electrospray ionization with FT-ICR MS and Orbitrap-MS. Fuel 282, 118790. https://doi.org/10.1016/j.fuel.2020.118790.
Wan, Z.H., Li, S.M., Pang, X.Q., et al., 2017. Characteristics and geochemical significance of heteroatom compounds in terrestrial oils by negative-ion electrospray Fourier transform ion cyclotron resonance mass spectrometry. Org. Geochem. 111, 34–55. https://doi.org/10.1016/j.orggeochem.2017.05.009.
Wang, Q., Hao, F., Cao, Z.C., et al., 2021. Heteroatom compounds in oils from the Shuntuoguole low uplift, Tarim Basin characterized by (+ESI) FT-ICR MS: implications for ultra-deep petroleum charges and alteration. Mar. Petrol. Geol. 134, 105321. https://doi.org/10.1016/j.marpetgeo.2021.105321.
Wang, W., Dong, M., Song, C.X., et al., 2018. Structural information of asphaltenes derived from petroleum vacuum residue and its hydrotreated product obtained by FT-ICR mass spectrometry with narrow ion isolation windows. Fuel 227, 111–117. https://doi.org/10.1016/j.fuel.2018.04.064.
Zhan, D.L., Fenn, B.J., 2000. Electrospray mass spectrometry of fossil fuels. Int. J. Mass Spectrom. 194 (2–3), 197–208. https://doi.org/10.1016/S1387-3806(99)00186-4.
Ziegs, V., Noah, M., Poetz, S., et al., 2018. Unravelling maturity-and migration-related carbazole and phenol distributions in Central Graben crude oils. Mar. Petrol. Geol. 94, 114–130. https://doi.org/10.1016/j.marpetgeo.2018.03.039.